Flight Test Results

The improved stability augmentation system was flight tested in the January–August period of 1967 by both Boeing and Air Force test pilots. The summary curve, Fig. 9, shows the Dutch roll damping and frequency obtained with the prototype system as well as the Dutch roll criteria utilized for the SAS development. The pilots' comments during the test program were highly favorable in regard to the damping provided by the SAS in both the longitudinal and lateral-directional axis. The flying qualities of the airplane were also improved due to the addition of the hydraulically powered elevator and rudder, which improved the control authority as well as improving the preciseness of control input.

A summary checklist of the effect of the stability augmentation system on flying qualities is given in Table 3. This table depicts how each element of the new stability augmentation system affected the flying qualities.

The increase in rudder power was accompanied with a reduction in pedal force gradient which significantly improved the control harmony. The increase in elevator control power throughout the flight envelope also provided a significant improvement in the flying qualities. The improvement in control linearity also makes it possible to use more finesse in the landing pattern and at touchdown. Manual refueling performance is also improved because the pilot has a decreased tendency to overcontrol.

The improvement in Mach buffet characteristics can be attributed to two effects of the powered elevator; first, the effects of the tab feedback to the column has been eliminated which reduces the column shake due to Mach buffet; and second, the elevator deflection is maintained constant by the actuator eliminating an elevator condition associated with the present tab configuration which, in turn, causes a large g influence due to Mach buffet. The flight test results showed that the improved stability augmentation system would significantly improve the airplane structural characteristics (Ref. 1) and also enhance the airplane flying qualities.

References

[1] Dempster, J. B. and Arnold, J. I., "Flight Test Evaluation of an Advanced Stability Augmentation System for the B-52 Aircraft," AIAA Paper 68-1068, Philadelphia, Pa., 1968.

[2] "Military Specification—Flying Qualities of Piloted Airplanes," MIL-F-008785, Oct. 1968, U.S. Air Force.

[3] Arnold, J. I., "Automatic Control for Damping Large Aircraft Elastic Vibrations," Paper, National Aeronautical Electronics Conference.

[4] Dempster, J. B. and Roger, K. L., "Evaluation of B-52 Structural Response to Random Turbulence With Various Stability Augmentation System," *Journal of Aircraft*, Vol. 4, No. 6, Nov.–Dec. 1967, pp. 507–512.

NOV.-DEC. 1969 J. AIRCRAFT VOL. 6, NO. 6

Simplified Design Equations for Buckling of Axially Compressed Sandwich Cylinders with Orthotropic Facings and Core

C. D. Reese* and C. W. Bert†
University of Oklahoma, Norman, Okla.

In this paper, the linear theory for buckling of axially compressed orthotropic sandwich cylinders presented in Ref. 1 is investigated in terms of various material parameters utilizing a high-speed digital computer. Simplified design equations which approximate this theory are then presented. The accuracy of these simplified design equations is compared with that of the other available approximations using the analysis of Ref. 1 as a basis.

Nomenclature

a_i = coefficients defined in Eqs. (2)
c = core depth
D_x, D_y, D_{xy} = flexural rigidities of orthotropic sandwich shell
D_{qx}, D_{qy} = transverse shear rigidities of orthotropic core material
E_x, E_y = Young's moduli of the facings in the x and y directions
G_{xy} = shear modulus of orthotropic facings
G_{xz}, G_{yz} = shear moduli of the core in the xz and yz planes
h = $c + t$
K = dimensionless buckling parameter
L = axial length of cylinder
m = $m_1\pi/L$
m_1 = axial wave number
N_x = axial force resultant
N = $-N_x$
n = $n_1/2R$
n_1 = circumferential wave number
R = radius of middle surface of cylinder
S_x, S_y, S_{xy} = stretching rigidities of orthotropic sandwich shell
t = facing thickness
ν_{xy}, ν_{yx} = facing Poisson's ratios
σ_{cr} = maximum fiber stress in facings at which buckling occurs in a cylinder subject to axial compression

Subscripts

cr = used to indicate critical buckling
rc = used to denote rigid core
x,y,z = coordinates on the cylinder middle surface in the axial, circumferential, and normal directions, respectively

Received November 1, 1968; revision received March 19, 1969.

* Graduate Student, School of Aerospace and Mechanical Engineering.

† Professor, School of Aerospace and Mechanical Engineering. Associate Fellow AIAA.

1. Introduction

Reference 1 presented a linear general-instability analysis of an axially compressed sandwich cylindrical shell having both facings and core of arbitrary orthotropy.

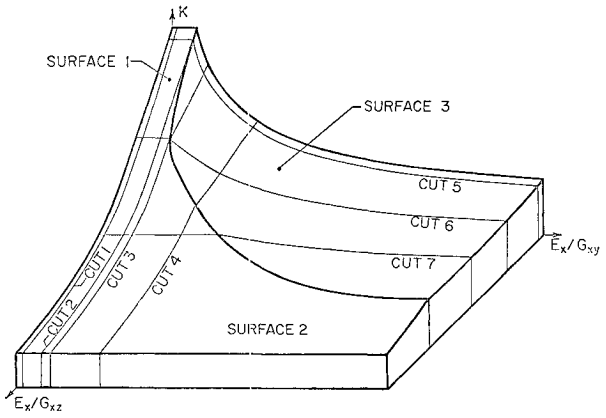

Fig. 1 Buckling surface for an axially compressed sandwich cylinder with orthotropic facings and core.

Previous linear analyses were for special cases only: isotropic facings and core,[2] isotropic facings and unidirectional core,[2] isotropic facings and orthotropic core,[3] and orthotropic facings and rigid core ($G_{xz}^{-1} = G_{yz}^{-1} = 0$).[4]

The buckling analysis of Ref. 1 was based on the sandwich-shell theory of Stein and Mayers,[5] with an additional simplifying assumption that the corresponding Poisson's ratios for bending and extension are equal. Later Peterson[6] presented a buckling analysis based on Ref. 5, but without this simplifying assumption. However, in practice, the effect of this simplifying assumption is not restrictive.

Results were given in Ref. 1 for the set of material parameters corresponding to the test cylinders. In this paper, the analysis of Ref. 1 is investigated in terms of various material parameters using a computer. Simplified design equations are presented to permit a designer to determine approximate buckling stresses without the aid of a computer.

2. Linear Buckling Analysis

The critical buckling stress under uniform axial compression for a sandwich circular cylindrical shell having simply supported edges and orthotropic facings and core can be expressed as follows.[1]

$$\sigma_{cr} = N_{cr}/2t = (a_0 + a_1)/2t \tag{1}$$

where

$$a_0 = (a_2^2 a_6 + a_3^2 a_5 - 2a_2 a_3 a_4)(a_4^2 - a_5 a_6)^{-1} m^{-2}$$

$$a_1 = m^{-2}\{D_x m^4 + 2(\nu_{yx} D_x + D_{xy}) m^2 n^2 + D_y n^4 + (S_x S_y m^4/R^2)[S_x m^4 + (S_x S_y S_{xy}^{-1} - 2\nu_{xy} S_y) m^2 n^2 + S_y n^4]^{-1}\}$$

$$a_2 = D_x m^3 + (\nu_{yx} D_x + D_{xy}) m n^2 \tag{2}$$

$$a_3 = D_y n^3 + (\nu_{xy} D_y + D_{xy}) m^2 n$$

$$a_4 = [(\nu_{xy} D_y) + (D_{xy}/2)] m n$$

$$a_5 = D_{qx} + D_x m^2 + (D_{xy}/2) n^2$$

$$a_6 = D_{qy} + D_y n^2 + (D_{xy}/2) m^2$$

The composite shell stiffnesses are calculated as follows:

$$S_x = 2tE_x,\ S_y = 2tE_y,\ S_{xy} = 2tG_{xy}$$

$$D_x = h^2 S_x/4(1 - \nu_{xy}\nu_{yx}),\ D_y = h^2 S_y/4(1 - \nu_{xy}\nu_{yx}) \tag{3}$$

$$D_{xy} = h^2 S_{xy}/2$$

and the core stiffnesses by the following expressions:

$$D_{qx} = G_{xz}(c + t)^2/c,\ D_{qy} = G_{yz}(c + t)^2/c \tag{4}$$

Equation (1) can be rewritten in terms of K, the theoretical buckling coefficient, as

$$\sigma_{cr} = (KE_x h/R)[1 - \nu_{xy}\nu_{yx}]^{-1/2} \tag{5}$$

Combining Eqs. (1) and (5),

$$K = [(a_0 + a_1)R/(2tE_x h)][1 - \nu_{xy}\nu_{yx}]^{1/2} \tag{6}$$

Even though Eq. (6) could be minimized with respect to the wave parameters m_1 and n_1, a solution to the resulting equations is not apparent except in the axisymmetric case where $n_1 = 0$. One alternative method of solution is to calculate the critical buckling coefficient for all practical integer combinations of m_1 and n_1. The lowest such value would then correspond to the actual critical stress. Such a solution is feasible only with the aid of a high-speed computer.

3. Discussion of Numerical Results

In order to determine the interaction between core and facing shear flexibilities, a numerical analysis was undertaken in which all of the parameters, except G_{xy}, G_{xz}, and G_{yz} were held constant. In this analysis, the core shear moduli G_{xz} and G_{yz} were kept at a constant ratio typical of honeycomb core material. The fixed parameters corresponded to the composite shells reported in Ref. 1 with the exception of shear moduli. The fixed parameters used were as follows: E_x = 3,280,000 psi, E_y = 3,140,000 psi, ν_{xy} = 0.13, t = 0.02 in., R = 21.94 in., c = 0.30 in., L = 72 in., and G_{yz}/G_{xz} = 0.572.

The resulting values of the buckling coefficient K can be depicted as a function of the dimensionless moduli ratios E_x/G_{xz} and E_x/G_{xy} by the three-dimensional surface shown in Fig. 1. Figures 2 and 3 show various cutting planes through the surface.

The surface shown in Fig. 1 consists of three distinct regions or subsurfaces. These regions are as follows: surface 1, axisymmetric facing mode of buckling; surface 2, axisymmetric core shear buckling mode; and surface 3, nonsymmetric facing buckling mode.

The axisymmetric facing buckling mode, shown as surface 1, can be found by setting $n = 0$ in Eq. (1). The resulting equation can then be minimized with respect to the axial wave parameter such that

$$\sigma_{cr} = \frac{h}{R}\left[\frac{E_x E_y}{1 - \nu_{xy}\nu_{yx}}\right]^{1/2}\left[1 - \frac{ct}{2hR}\left(\frac{E_x E_y/G_{xz}^2}{1 - \nu_{xy}\nu_{yx}}\right)^{1/2}\right] \tag{7}$$

This agrees with the findings of Ref. 7 for the axisymmetric case. Then Eq. (5) becomes

$$K = \left(\frac{E_y}{E_x}\right)^{1/2}\left[1 - \frac{ct}{2hRG_{xz}}\left(\frac{E_x E_y}{1 - \nu_{xy}\nu_{yx}}\right)^{1/2}\right] \tag{8}$$

This mode of buckling is primarily a function of E_x and E_y, and secondarily a function of G_{xz}.

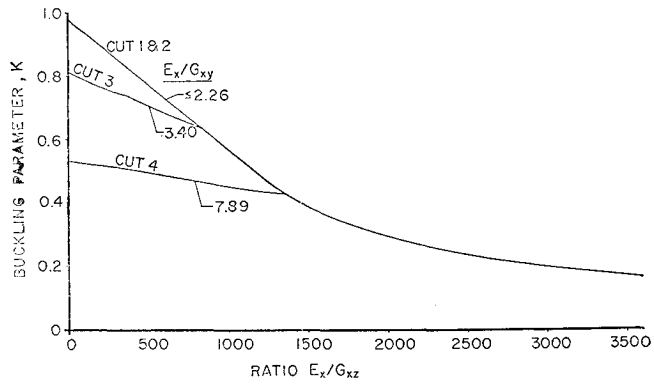

Fig. 2 Plot of buckling parameter K vs ratio of E_x/G_{xz}.

The axisymmetric core shear buckling mode, surface 2, occurs when $n_1 = 0$ and m_1 becomes very large. Then Eq. (1) reduces to the following:

$$\sigma_{cr} = D_{qx}/2t = G_{xz}h^2/2ct \tag{9}$$

Equation (9) can be further simplified for a sandwich cylinder with very thin facings by noting that c is approximately equal to h in that case. Then Eq. (9) becomes

$$\sigma_{cr} = G_{xz}h/2t \tag{10}$$

This is the same result as was reported in Ref. 8 for the case in which buckling occurs by the faces sliding relative to one another (crimping). As seen by Eqs. (9) and (10), the core shear mode (crimping mode) is a function of only one material property G_{xz}.

The nonsymmetric facing buckling mode is primarily a function of G_{xy} and secondarily a function of G_{xz}. This is the most complicated type of buckling and no simplifications of the general solution are apparent. It is important to note that this buckling mode cannot take place in shells with isotropic facings, yet it is the most predominant buckling mode in the case of facings of composite materials, since they usually have high values of E_x/G_{xy}.

In the example used here, the line separating surfaces 1 and 2 is not obvious due to the smooth transition between modes. For this case, it occurs at an E_x/G_{xz} ratio of approximately 1100. For other choices of the material and geometrical parameters, a more distinct transition might occur.

Figure 2 shows various cuts through the buckling surface parallel to the E_x/G_{xz} axis. It is apparent from this figure that any plane parallel to the E_x/G_{xz} axis will reveal identical curves for the axisymmetric modes (surfaces 1 and 2). This corresponds to cuts 1 and 2 shown in Fig. 2. Although this axisymmetric buckling line provides a bound on buckling, it is an upper bound to the nonsymmetric mode and is of little interest in this regard.

Cut 4 shown in Fig. 2 is based upon an actual set of material and geometrical parameters and thus helps to give some insight into the design aspects of the buckling surface. This curve was calculated for the facing material of Ref. 1. It shows the dependency of the buckling stress upon the core shear modulus.

It can also be noted in Fig. 2 that the curves have a double curvature in the axisymmetric facing (surface 1) and the nonsymmetric facing (surface 3) buckling regions. This characteristic is probably due to different terms in Eqs. (1) and (2) predominating for different ranges of G_{xz}.

Figure 3 shows the cuts through the surface parallel to the E_x/G_{xy} axis. The axisymmetric regions (surfaces 1 and 2) show up here as straight horizontal lines. Again this emphasizes the independence of G_{xy} in the axisymmetric regions.

4. Simplified Design Equations

Since the designer must normally make numerous calculations before arriving at the optimal design in terms of material and geometrical parameters, a computer solution such as used here is of little value except possibly to check the final design. With this in mind, an attempt has been made to approximate this more complicated analysis with a set of design equations which can be solved without the aid of a high-speed computer.

It must be pointed out that the solution discussed here considers generally instability only and the final design must also be checked for column buckling and face dimpling or wrinkling. It is recommended that the designer follow the procedure outlined in Ref. 9, except that the equations presented here should be substituted for the general instability portion of the analysis.

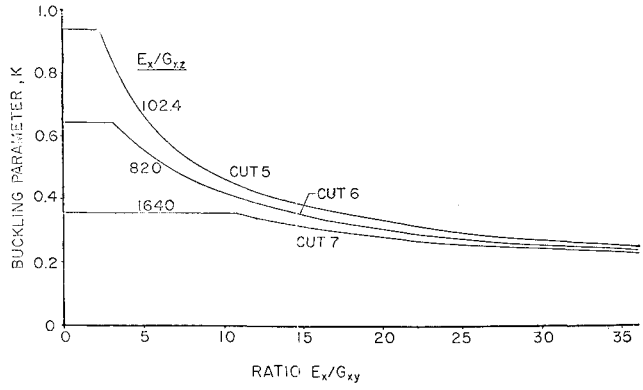

Fig. 3 Plot of buckling parameter K vs ratio of E_x/G_{xy}.

Allowing G_{xz} to become large in Eq. (7) results in the rigid-core axisymmetric solution

$$(\sigma_{cr})_{rc} = (h/R)[E_xE_y/(1 - \nu_{xy}\nu_{yx})]^{1/2} \tag{11}$$

Then Eq. (7) can be rewritten in the following form:

$$\sigma_{cr} = (\sigma_{cr})_{rc}\left[1 - \frac{1}{2}\frac{(\sigma_{cr})_{rc}tc}{G_{xz}h^2}\right] \tag{12}$$

Since Eq. (11) was found from an axisymmetric solution, the effect of facing shear is not present. Reference 4 presented a rigid-core analysis for the nonsymmetric mode of buckling in which the equation analogous to Eq. (11) was found to be

$$(\sigma_{cr})_{rc}^* = \frac{2t}{R}\left[\left(1 + \frac{c}{2t}\right)^3 - \left(\frac{c}{2t}\right)^3\right]^{1/2} \times \left[\frac{E_xE_y}{3(1 - \nu_{xy}\nu_{yx})}\right]^{1/2}\Phi \tag{13}$$

where Φ is given as $\Phi = 1$, or

$$\Phi = \left[\frac{2G_{xy}[1 + (\nu_{xy}\nu_{yx})^{1/2}]}{(E_xE_y)^{1/2}}\right]^{1/2}$$

whichever is smaller.

For a sandwich cylinder that has thin facings in comparison with the core thickness, it can be shown by expanding the radical that

$$h \simeq \frac{2t}{(3)^{1/2}}\left[\left(1 + \frac{c}{2t}\right)^3 - \left(\frac{c}{2t}\right)^3\right]^{1/2}$$

Thus, Eqs. (13) and (11) are essentially the same for the axisymmetric case ($\Phi = 1$). This suggests that if Eq. (13) is combined with Eq. (12), the resulting solution would provide a simple approximation which could be utilized in the nonsymmetric buckling region. Then

$$\sigma_{cr} = \Phi(\sigma_{cr})_{rc}\{1 - 1/2[\Phi(\sigma_{cr})_{rc}tc/G_{xz}h^2]\} \tag{14}$$

Since a simple solution is already available for the core shear mode of buckling, Eq. (9), it is necessary only to determine which equation should be used for any particular set of design parameters. By comparing Eqs. (9) and (12), a simple criterion was found for determining which equation to use: 1) if the estimated stress given by Eq. (14) is less than one-half of the rigid-core buckling stress, Eq. (13), then Eq. (9) should be used for estimating the critical stress; 2) otherwise, Eq. (14) gives the critical estimate.

To determine how good of an estimate the simplified method suggested above provides, the critical stresses as calculated by the simplified equation for several facing materials were compared to the results of the improved theory, Eqs. (1) and (2), using a computer. The best available analysis prior to this time was provided by the rigid-core analysis of Ref. 4. The results obtained by the rigid-core analysis were also compared

Table 1 Comparison of error in estimates of buckling coefficient for honeycomb-core cylinders with facings of 181-style cloth E-glass/epoxy

Facing properties (Ref. 1)
$E_x = 3.28 \times 10^6$ psi $G_{xy} = 0.416 \times 10^6$ psi
$E_y = 3.14 \times 10^6$ psi $\nu_{xy} = 0.13$

	Critical stress				
	Linear analysis (Ref. 1),	Present estimate Eqs. (9) and (14),		Rigid-core analysis Eq. (13),	
E_x/G_{xz}	psi	psi	% error	psi	% error
3280	8540	8540	0	25510	−198.7
1640	17100	15977	6.6	25510	−49.2
1093	21269	19155	9.9	25510	−19.9
820	22325	20744	7.1	25510	−14.3
547	23591	22333	5.3	25510	−8.1
273.5	24756	23922	3.4	25510	−3.0
164.2	25089	24557	2.1	25510	−1.7
102.4	25285	24915	1.5	25510	−0.9
65.6	25406	25129	1.0	25510	−0.4
6.56	25606	25472	0.5	25510	0.4

Table 2 Comparison of error in estimates of buckling coefficient for honeycomb-core cylinders with facings of unidirectional S-glass/epoxy oriented in longitudinal direction

Facing properties (Ref. 11)
$E_x = 8.4 \times 10^6$ psi $G_{xy} = 0.9 \times 10^6$ psi
$E_y = 1.8 \times 10^6$ psi $\nu_{xy} = 0.29$

	Critical stress				
	Linear analysis (Ref. 1),	Present estimate Eqs. (9) and (14),		Rigid-core analysis Eq. (13),	
E_x/G_{xz}	psi	psi	% error	psi	% error
8400	8540	8540	0	41471	−385.6
4200	17080	17080	0	41471	−142.8
933.3	38735	35872	7.4	41471	−7.1
420	40611	38951	4.1	41471	−2.1
262.5	41146	39896	3.0	41471	−0.8
168	41451	40463	2.4	41471	0
84	41729	40967	1.8	41471	0.6
16.8	41956	41370	1.4	41471	1.2

with the improved theory results. This information is tabulated in Tables 1–7 for facings of epoxy reinforced with 181-style E-glass cloth (cut 4 in Figs. 1 and 2), unidirectional S-glass oriented longitudinally, unidirectional S-glass oriented circumferentially, unidirectional boron oriented longitudinally, unidirectional boron oriented circumferentially, unidirectional Thornel oriented longitudinally, and unidirectional Thornel oriented circumferentially. The geometric parameters used were the same as used before.

Table 3 Comparison of error in estimate of buckling coefficient for honeycomb-core cylinders with facings of unidirectional S-glass/epoxy oriented in circumferential direction

Facing properties (Ref. 11)
$E_x = 1.8 \times 10^6$ psi $G_{xy} = 0.9 \times 10^6$ psi
$E_y = 8.4 \times 10^6$ psi $\nu_{yx} = 0.29$

	Critical stress				
	Linear analysis (Ref. 1),	Present estimate Eqs. (9) and (14),		Rigid-core analysis Eq. (13),	
E_x/G_{xz}	psi	psi	% error	psi	% error
1800	8540	8540	0	41471	−385.6
900	17080	17080	0	41471	−142.8
200	35379	35872	−1.4	41471	−17.2
90	38561	38951	−1.0	41471	−7.5
56.3	39693	39896	−0.5	41471	−4.5
36	40454	40463	0	41471	−2.5
18	41168	40967	0.5	41471	−0.7
3.6	41787	41370	1.0	41471	0.8

Table 4 Comparison of error in estimates of buckling coefficient for honeycomb-core cylinders with facings of unidirectional boron/epoxy oriented in longitudinal direction

Facing properties (Ref. 10)
$E_x = 3.0 \times 10^7$ psi $G_{xy} = 1.1 \times 10^6$ psi
$E_y = 3.0 \times 10^6$ psi $\nu_{xy} = 0.38$

	Critical stress				
	Linear analysis (Ref. 1),	Present estimate Eqs. (9) and (14),		Rigid-core analysis Eq. (13),	
E_x/G_{xz}	psi	psi	% error	psi	% error
30000	8540	8540	0	71037	−731.8
15000	17080	17080	0	71037	−315.9
3333	64202	54610	14.9	71037	−10.6
1500	64498	63645	7.1	71037	−3.7
938	69418	66417	4.3	71037	−2.3
600	69998	68080	2.7	71037	−1.5
300	70531	69559	1.4	71037	−0.7
60	70971	70741	0.3	71037	−0.1

Table 5 Comparison of error in estimates of buckling coefficient for honeycomb-core cylinders with facings of unidirectional boron/epoxy oriented in the circumferential direction

Facing properties (Ref. 10)
$E_x = 3.0 \times 10^6$ psi $G_{xy} = 1.1 \times 10^6$ psi
$E_y = 3.0 \times 10^7$ psi $\nu_{yx} = 0.38$

	Critical stress				
	Linear analysis (Ref. 1),	Present estimate Eqs. (9) and (14),		Rigid-core analysis Eq. (13),	
E_x/G_{xz}	psi	psi	% error	psi	% error
3000	8540	8540	0	71037	−731.8
1500	17080	17080	0	71037	−315.9
333.3	50397	54610	−8.4	71037	−41.0
150	60294	63645	−5.6	71037	−17.8
93.8	64361	66417	−3.2	71037	−10.4
60	67162	68080	−1.4	71037	−5.8
30	68977	69559	−0.8	71037	−3.0
6	70649	70741	−0.1	71037	−0.5

The negative values shown in the tables indicate an unconservative error, whereas positive values represent conserva-

Table 6 Comparison of error in estimates of coefficient for honeycomb-core cylinders with facings of unidirectional Thornel[a] 40/828-1031 epoxy oriented in longitudinal direction

Facing properties (Ref. 12)
$E_x = 24.0 \times 10^6$ psi $G_{xy} = 0.85 \times 10^6$ psi
$E_y = 0.89 \times 10^6$ psi $\nu_{xy} = 0.39$

	Critical stress				
	Linear analysis (Ref. 1),	Present estimate Eqs. (9) and (14),		Rigid-core analysis Eq. (13),	
E_x/G_{xz}	psi	psi	% error	psi	% error
24000	8540	8540	0	42510	−397.8
12000	17080	17080	0	42510	−148.9
2667	40486	36628	9.5	42510	−5.0
1200	42017	39863	5.1	42510	−1.2
750	42535	40856	3.9	42510	0.1
480	42858	41451	3.3	42510	0.8
240	43154	41981	2.7	42510	1.5
48	43362	42404	2.2	42510	2.0

[a] Thornel is a registered trademark of Union Carbide Corporation for graphite yarn.

Table 7 Comparison of error in estimate of buckling coefficient for honeycomb-core cylinders with facings of unidirectional Thornel[a] 40/828-1031 epoxy oriented in circumferential direction

Facing properties (Ref. 12)
$E_x = 0.89 \times 10^6$ psi $G_{xy} = 0.85 \times 10^6$ psi
$E_y = 24.0 \times 10^6$ psi $\nu_{yx} = 0.39$

	Critical stress				
	Linear analysis (Ref. 1),	Present estimate Eqs. (9) and (14),		Rigid-core analysis Eq. (13),	
E_x/G_{xz}	psi	psi	% error	psi	% error
890.0	8540	8540	0	42510	−397.8
445.0	17080	17080	0	42510	−148.9
98.9	31420	36628	−16.6	42510	−35.3
44.5	36760	39863	−8.4	42510	−15.6
27.8	38663	40856	−5.7	42510	−10.0
15.1	40037	41451	−3.5	42510	−6.2
8.9	41500	41981	−1.2	42510	−2.4
1.51	42888	42404	1.1	42510	0.9

[a] Thornel is a registered trademark of Union Carbide Corporation for graphite yarn.

tive variations. As expected, the rigid-core analysis is normally unconservative. In those few cases where it is unconservative, Tables 3, 5, and 7, it is considerably closer than the rigid-core analysis. All of the points in the tables are for values in the nonsymmetric mode and the axisymmetric core shear mode regions. There was no necessity to calculate data for the axisymmetric facing buckling mode, since the equations compared here must agree in this area due to the bases of the formulation.

5. Conclusion

Although no attempt is made to imply that the approximation presented in this paper is as accurate as the improved analysis of Ref. 1, the approximation is of a simple enough form that many design parameters can be varied without excessive computation. Even when a computer is readily available for solving Eqs. (1) and (2), it would appear to be more feasible economically to use the approximate analysis presented here for all preliminary design computations and to use the exact analysis only for a final design check.

References

[1] Bert, C. W., Crisman, W. C., and Nordby, G. M., "Buckling of Cylindrical and Conical Sandwich Shells with Orthotropic Facings," *AIAA Journal*, Vol. 7, No. 2, Feb. 1969, pp. 250–257.

[2] Stein, M. and Mayers, J., "Compressive Buckling of Simply Supported Curved Plates and Cylinders of Sandwich Construction," TN 2601, Jan. 1952, NACA.

[3] Zahn, J. J. and Kuenzi, E. W., "Classical Buckling of Cylinders of Sandwich Construction in Axial Compression—Orthotropic Cores," Rept. FPL-018, Nov. 1963, Forest Products Lab., Madison, Wis.

[4] Dow, N. F. and Rosen, B. W., "Structural Efficiency of Orthotropic Cylindrical Shells Subjected to Axial Compression," *AIAA Journal*, Vol. 4, No. 3, March, 1966, pp. 481–485.

[5] Stein, M. and Mayers, J., "A Small-Deflection Theory for Curved Sandwich Plates," Rept. 1008, 1952, NACA.

[6] Peterson, J. P., "Plastic Buckling of Plates and Shells Under Biaxial Loading," TN D-4706, Appendix D, Aug. 1968, NASA.

[7] Peterson, J. P. and Anderson, J. K., "Structural Behavior and Buckling Strength of Honeycomb Sandwich Cylinders Subjected to Bending," TN D-2926, Aug. 1965, NASA.

[8] Cunningham, J. H. and Jacobson, M. J., "Design and Testing of Honeycomb Sandwich Cylinders Under Axial Compression," *Collected Papers on Instability of Shell Structures*, TN D-1510, Dec. 1962, NASA, pp. 341–352.

[9] *Structural Sandwich Composites*, MIL-HDBK-23A, Dept. of Defense, Washington, D.C., Dec. 1968, Chap. 12.

[10] Waddoups, M. E., "Characterization and Design of Composite Materials," *Composite Materials Workshop*, edited by S. W. Tsai, J. C. Halpin and N. J. Pagano, Technomic Publishing Co. Inc., Stamford, Conn., 1968, pp. 254–308.

[11] Ekvall, J. C., "Structural Behavior of Monofilament Composites," *AIAA 6th Structures and Materials Conference*, AIAA, New York, April 1965, pp. 250–263.

[12] Novak, R. C., "Investigation of Graphite Filament Reinforced Epoxies," Publication U-4379, May 1968, Aeronutronic Div., Philco-Ford Corp., Newport Beach, Calif.